metals

MDPI

Article

Fabrication of Functionally Graded Materials Using Aluminum Alloys via Hot Extrusion

Dasom Kim [1], Kwangjae Park [1], Minwoo Chang [2], Sungwook Joo [3], Sanghwui Hong [3], Seungchan Cho [4] and Hansang Kwon [1,5,*]

1 Department of Materials System Engineering, Pukyong National University, 365, Sinseon-ro, Nam-gu, Busan 48547, Korea; ds09262000@naver.com (D.K.); pkj3678@naver.com (K.P.)
2 Department of Research and Development, Daeyeong Metal. Co., Ltd., 1209-7 SinSang-ri Jinryang-eup, Kyungsan 38470, Korea; ngm01@ngm.re.kr
3 Department of Converged Technology Research, Gyeongbuk Hybrid Technology Institute, Goiyean-dong, Yeongcheon, Gyeongbuk 38899, Korea; ngm06@ngm.re.kr (S.J.); ngm05@ngm.re.kr (S.H.)
4 Department of Composites Research, Korea Institute of Materials Science, Changwon-daero, Seongsan-gu, Changwon-si, Gyeongsangnam-do 51508, Korea; seungchan.cho@gmail.com
5 Department of Research and Development, Next Generation Material Co., Ltd., 365, Sinseon-ro, Nam-gu, Busan 48547, Korea
* Correspondence: kwon13@pknu.ac.kr; Tel.: +82-51-629-6383

Received: 20 December 2018; Accepted: 7 February 2019; Published: 11 February 2019

Abstract: In this study, we have attempted to manufacture functionally graded materials (FGMs) using aluminum alloys 3003 and 6063 via a hot extrusion process to realize multifunctionality through achieving high strength and low weight. The FGMs were fabricated using Al3003 powder and Al6063 bulk to improve the interfacial properties. Particle size analysis and X-ray fluorescence of the Al3003 powder were used to analyze the composition of general Al3003; microstructure analysis revealed improved hardness with almost no defects, such as cracks at the interface between the two materials. The experimentally determined tensile strength of the composite was observed to be higher than the theoretical value calculated using the rule of mixtures; the strengthening mechanisms considered for the calculations were grain size reduction and precipitation hardening. In particular, we attempted to predict the strengthening effect resulting from the fine grain size of the powder and grain size reduction due to the extrusion process using the Hall–Petch equation. The Kelly–Tyson equation was also used to calculate the theoretical strength in the presence of the strengthening phases. Based on these results, it was confirmed that FGMs can be successfully produced using the hot extrusion process.

Keywords: functionally graded materials (FGMs); aluminum alloy; hot extrusion; Hall–Petch equation; Kelly–Tyson equation

1. Introduction

Lightweight materials have been extensively developed for use in transport machineries, especially in aircrafts, automobiles, and marine vehicles. In particular, aluminum is generally used to realize lightweight in materials. Therefore, aluminum has been used in the form of an alloy by adding other elements by many researchers, such as Al-Stainless steel (SUS) composite and Al-carbon nanotubes (CNT) composite [1–3].

Recently, multifunctionality, where diverse functions are realized in the same material, has been increasingly desired. In this context, the concept of functionally graded materials (FGMs) has been suggested as a method to realize multifunctionality. FGMs are materials in which a gradient in property is created by changing the composition continuously.

Miyamoto et al. introduced the concept of FGMs [4]. This concept facilitates the improvement of the quality of the interfaces in a heterogeneous material to prevent cracks, which arise due to the residual stress resulting from the difference in the properties of the different components in the heterogeneous material.

The FGMs mitigate the differences in the properties between the two materials by forming interlayers; however, this is difficult to control because the layers formed at the interface must be thin and uniform. Besides, cracks are sometimes also observed in the FGMs.

To address these problems, researchers have attempted new fabrication methods, such as centrifugal casting, semi-solid forming under magnetic field, and spark plasma sintering (SPS) [5–7], while extrusion processes such as co-extrusion, indirection, and constant extrusion have been used as a fabrication method for over 30 years [8,9]. Fan et al. attempted to join Al1060 and Al6063 by welding following die extrusion [10]. However, there were many cracks at the interface due to the difficulty in controlling the stress. Kwon et al. tried a hot extrusion process to fabricate an Al-CNT composite [11]. The microstructure was observed to be elongated in a direction parallel to the direction of the extrusion, with no cracks and pores. Furthermore, although the composite includes only one volume, the mechanical properties were significantly improved.

This study attempted to fabricate FGMs via a hot extrusion process. The Al3003/Al6063 FGM fabricated in this study has the shape of a rod, the center axis of which consists of Al3003 and serves as a skeleton for the material; this center is surrounded by Al6063. While Al6063 is an aluminum-based alloy that has high strength and hardness to protect the material from external shock, the Al3003 alloy has excellent ductility, which gives flexibility to the material itself, thereby enhancing workability. Thus, the FGM is suitable for use as a wire material for an industrial electric pole and can also be used as a skeleton for steel structures or automobile structural materials.

For dissimilar materials to be well bonded, the surface area of the contact between the two materials must be large. For example, if the surface is rough and the bulk is in contact with a rugged bulk surface, the area of the contact will be larger. Uehara and Sakurai confirmed the relation between the bonding strength and surface roughness of a joined part, which was controlled by changing the feed in a common mechanical milling machine [12]. They observed that the tensile strength was higher when the surface roughness was increased to ~3–6 μm than when the surface roughness was <1 μm.

Figure 1a shows a schematic diagram of the contact surface between two materials in the bulk form. Under these conditions, the contact surface comprises the area indicated by the straight line where the two materials come into contact. On the other hand, if one material is bulk and the other is a powder (Figure 1b), the contact surface area significantly increases because the powder has a much larger surface area than the bulk. Furthermore, Figure 1c shows a schematic diagram of the contact surface between two materials in powder form. It can be observed that the surface area of the contact is much greater, although it is difficult to handle such bonding experimentally. Therefore, we fabricated the FGMs, as shown in Figure 1b; and expected better interface properties compared to the case when two bulk materials are used.

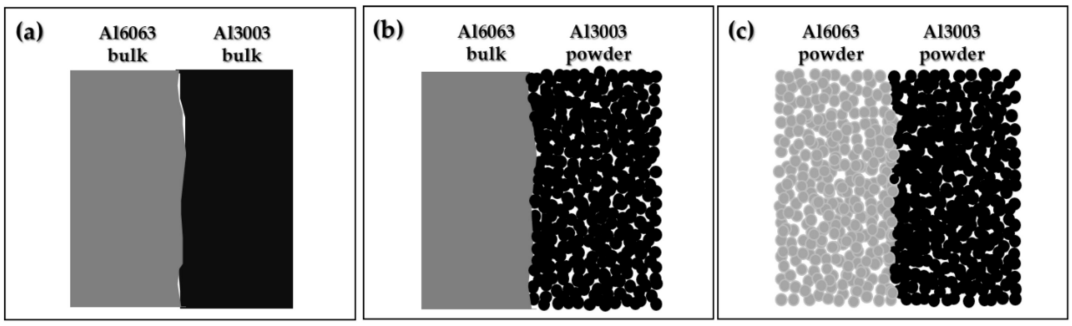

Figure 1. Illustration of the interface between two dissimilar materials. (**a**) bulk–bulk interface, (**b**) bulk–powder interface, and (**c**) powder–powder interface.

To fabricate a sample, we performed canning followed by extrusion. Subsequently, the microstructure of the sample was observed using scanning electron microscopy (SEM), and the composition of the FGMs was analyzed using energy-dispersive spectrometry (EDS). In addition, we used the value of the crystallite size, which was calculated using the Scherrer equation, in the Hall–Petch equation to elucidate the relation between the grain size and strength.

2. Materials and Methods

2.1. Sample Preparation

First, canning was performed as shown in Figure 2. Al3003 powder (965 g; ECKA Granules, purity: 99.5%, particle size: 100 μm) was poured into a bulk Al6063 can (outer diameter: 100 mm and inner diameter: 60 mm) and subjected to a vertical force under a pressure of 5000 kgf. Subsequently, the material was extruded at a temperature of 468 °C, which is below the melting point of both Al3003 and Al6063, using an extrusion machine (SKM Co., Ltd., Incheon, Korea). The temperatures of the billet, container, and mold were 468 °C, 407 °C, and 468 °C, respectively. The ram speed was 2.49 mm/s and the extrusion ratio was 100.

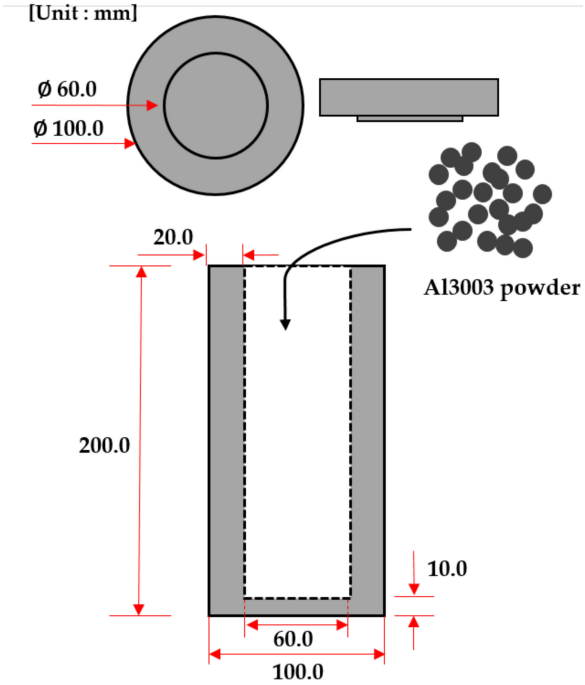

Figure 2. Schematic view of the Al6063 bulk cover and can.

2.2. Analysis of Raw Materials

Particle size analysis (PSA) and X-ray fluorescence (XRF) were used to characterize the Al3003 powder. PSA was first conducted (BECKMAN COULTER, LS 13 320, Indianapolis, IN, USA) followed by XRF to analyze the constituent elements (SHIMADZU, XRF-1800, Tokyo, Japan).

2.3. Characterization of the Samples

First, we used the Archimedes′ method to measure the density of the FGMs using a densitometer (KERN, ABJ 120-4M, Balingen, Germany). After etching with 5% NaOH solution, SEM and EDS were employed for a detailed analysis of a sectional area of the samples in detail (TESCAN, VEGA II LSU, city, Czech Republic). Elemental mapping was conducted to determine the ingredient elements of the material (TESCAN, VEGA II LSU, Brno, Czech Republic).

Subsequently, mechanical properties such as hardness and tensile strength were measured using the Vickers hardness test (HM-101, Mitutoyo Corporation, Kanagawa, Japan) according to JIS B 7725 and ISO 6507-2 at five points from the core to the clad (three measurements per point) with a load of 0.3 kg. To measure the tensile stress and strain, a tensile test was conducted on two FGM samples: Al3003/Al6063 FGMs without heat treatment (T-0) and T-5 heat-treated Al3003/Al6063 FGMs (Kyungdo precision Co., Ltd., Siheung, Korea). The no. 4 tensile specimen was fabricated according to KS B 0801 T-5 (width: 6 mm). The treatment is the process that artificially elevates the temperature of the specimen to 150–200 °C, and then cools it [13]. The tensile test was conducted at 24 °C using a 68.65 kN press. Finally, we used the Hall–Petch equation to confirm the relationship between the grain size and tensile strength; the grain size was substituted by the crystallite size, which was calculated using the Scherrer equation and the XRD data (Rigaku, Ultima IV, Tokyo, Japan). Furthermore, the Kelly–Tyson equation was used in this study to calculate the theoretical yield stress of the FGMs.

3. Results

In general, the dispersion of particle size is an important characteristic of a particulate sample and has significant influence on the packing density and porosity of the products.

Figure 3 shows the PSA graph of Al3003 powder with various particle sizes ranging from 10 μm to 280 μm; the average particle size is 125 μm. The accumulate volume graph also shows that the d_{10}, d_{50}, and d_{90} data for the particle size distribution is 35 μm, 97 μm, and 156 μm, respectively.

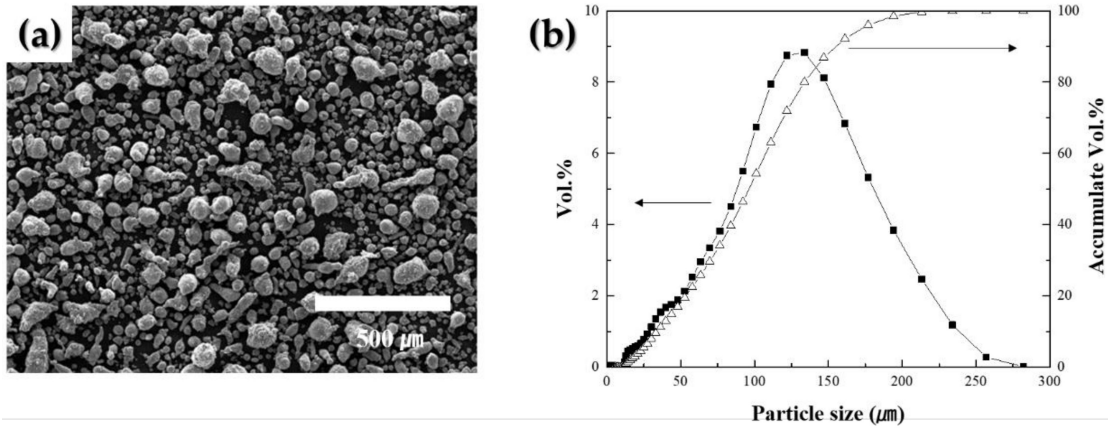

Figure 3. (**a**) scanning electron microscope (SEM) image of Al3003 powder and (**b**) Typical Particle size analysis (PSA) graph (black squares) and accumulate PSA graph (outlined triangles) of the Al3003 powder used in this study.

When Al3003 powder is filled into the Al6063 bulk can, a high packing density (about 63%) can be achieved as the Al3003 powder has a significantly high degree of dispersion in particle size, which indicates that the density of the FGMs is high.

Table 1 lists the general chemical composition of Al3003 and Al6063. By comparison, Si (1.10%), Mn (0.96%), Fe (0.87%), Zn (0.23%), Cu (0.17%), and Al (96.66%), which is determined by XRF, are present in the Al3003 powder used in this study.

Table 1. General chemical composition of the components Al6063 and Al3003 [14,15].

Material	Chemical Composition (%)									
	Si	Fe	Cu	Mn	Zn	Mg	Cr	Ti	Others	Al
Al6063	0.20–0.60	0.35	0.10	0.10	0.10	0.45–0.90	0.10	0.10	-	97.65–98.50
Al3003	0.6	0.7	0.05–0.20	1.0–1.5	0.10	-	-	-	-	96.90–97.55

We observe that the proportions of the components are approximately in the range of the typical chemical composition of the Al3003 powder (presented in Table 1). Consequently, Al3003 powder, with a mean particle size of 125 µm, was filled into a bulk can made of Al6063, and the final FGM was fabricated via hot extrusion.

Figure 4 shows the photograph of the final material, which is in the shape of a cylindrical rod. Figure 4b shows the cross-section of the FGM, where the inner darker area is composed of Al3003 and the outer brighter area is composed of Al6063. The inner diameter is around 1 mm, and the outer diameter is 8 mm. The density of the FGMs was also measured to confirm that there were nearly no flaws in the material manufactured via hot extrusion. The experimental density measured using the Archimedes' method was 2.6538 g/cm^3 and the theoretical density calculated using the rule of mixtures was 2.7009 g/cm^3. A significantly high relative density of 98.26% was obtained, which confirms the successful fabrication of a dense FGM. Furthermore, it was confirmed that the density of the Al3003 core was nearly 100%. This indicates that hot extrusion is a useful method to form an interface between powders and bulk materials, demonstrating that this process can be used for the fabrication of complex heterogeneous materials.

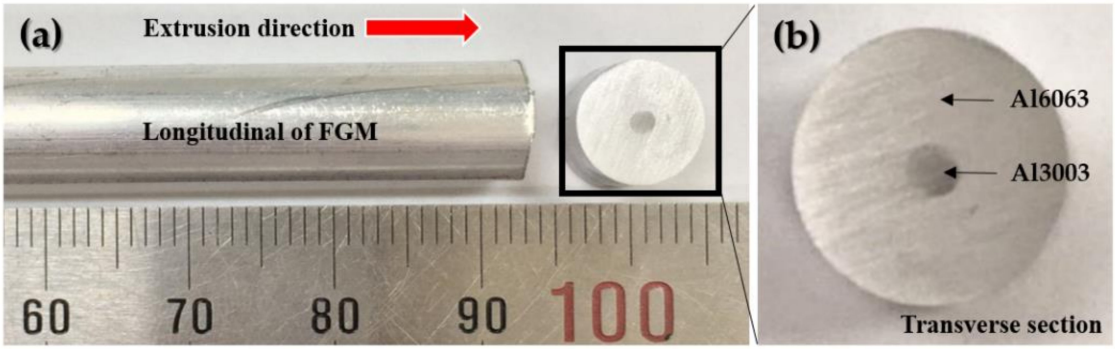

Figure 4. Al3003/Al6063 functionally graded materials (FGMs) fabricated via hot extrusion: (**a**) Photograph of the FGMs and (**b**) high-magnification image of the cross-section of Al3003/Al6063 FGMs.

Figure 5 shows the SEM images of the Al3003/Al6063 FGMs; microstructure analysis was performed to confirm whether the final FGM was fabricated without any cracks and faults. Figures 5d and 5f show the EDS results for Al6063 and Al3003.

By comparing the XRF results, where Mg and Si were determined to be the predominant components of Al6063 and Al3003, respectively, with the EDS result, we infer that Figure 5d corresponds to Al6063 and Figure 5f corresponds to Al3003.

There are no cracks, except for a few pores created via deep etching (Figure 5a) in the region containing Al6063. However, the Al3003 region consists of more pores, which was not observed before conducting the etching process, and moreover, particles were observed, as shown in Figure 5c. This could be because the etching process in Al3003 can be faster and more significant than in Al6063, since the Al3003 is in the form of a powder, which has a higher specific surface area, while Al6063 has higher corrosion resistance compared to Al3003. We also confirmed from the EDS results that the O content is higher in Al3003 than in Al6063. Hence, deep etching was required to observe the microstructure of Al6063, which has high corrosion resistivity. Therefore, these results show that oxidation has occurred more actively in Al3003 than in Al6063. Figure 5b shows the SEM micrograph of the interface between Al6063 and Al3003, demonstrating a distinct and well-formed interface without any flaws, such as cracks. Figure 5e shows a high-magnification micrograph, where no cracks can be observed, except for pores caused by the deep etching similar to Figure 5b.

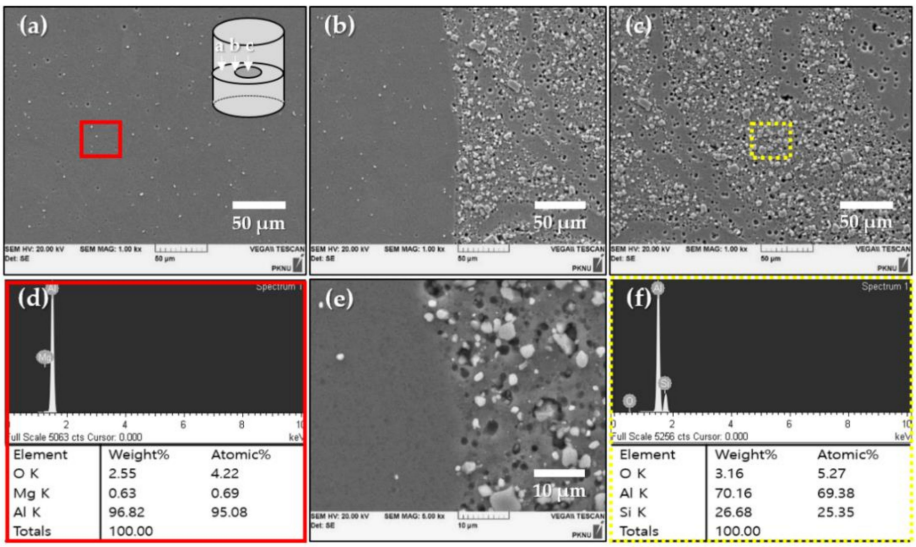

Figure 5. SEM images (**a**–**c**,**e**) and EDS results (**d**,**f**). (**a**) Region constituted by Al6063, (**b**) interface between Al6063 and Al3003, (**c**) region constituted by Al3003, (**d**) EDS of Al6063, (**e**) high-magnification image of the interfacial area between Al6063 and Al3003, and (**f**) EDS of Al3003.

Figure 6 shows the SEM image of a longitudinal section of the Al3003/Al6063 FGM. Figure 6a shows the region containing Al3003, where the pores are larger and longer when the extrusion direction was subjected to pressure and was compressed, whereas the longitudinal section parallel to the direction of extrusion was stretched in the same direction. The interface between Al3003 and Al6063 was analyzed in detail using elemental mapping.

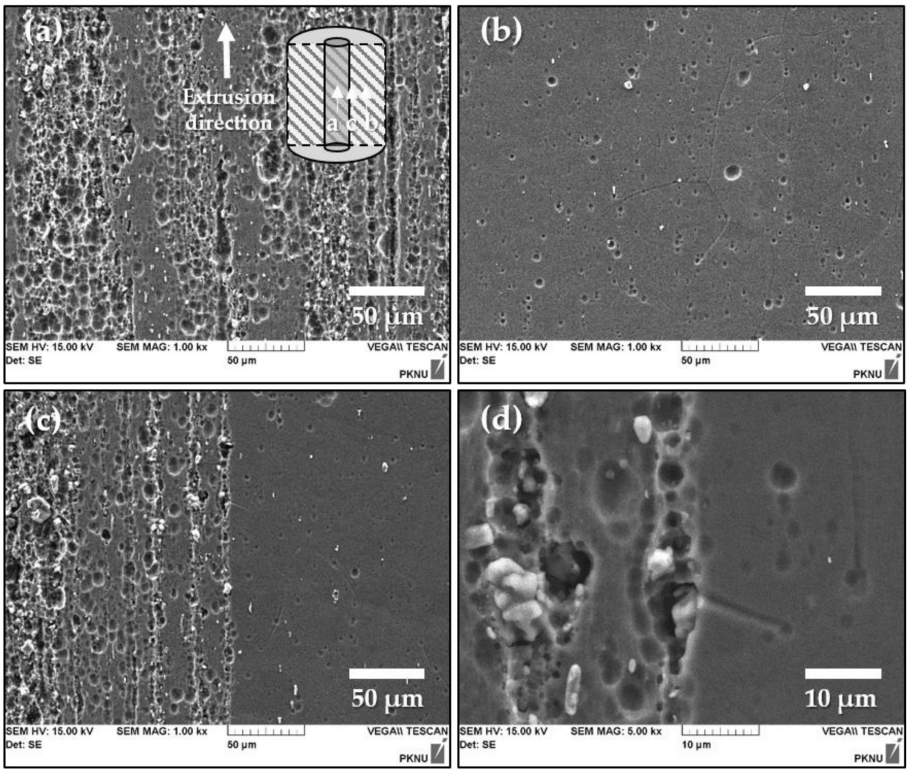

Figure 6. SEM images of the longitudinal section of the FGM. (**a**) Region containing Al3003, (**b**) region containing Al6063, (**c**) interface between Al3003 and Al6063, and (**d**) high-magnification image of the interface between Al3003 and Al6063.

Figure 7b shows the distribution of the relative concentrations of the different components at the interface between Al3003 and Al6063. The particles in the longitudinal section are observed to be relatively larger and have an elongated shape when compared with those observed in the cross-section. Therefore, we can consider that the grains of the FGMs are aligned in the direction of extrusion. Near the interface in the Al3003 area, we expect that the degree of oxidation caused by the deep etching is higher than in the other areas because of the higher O content and lower proportion of Al in this area.

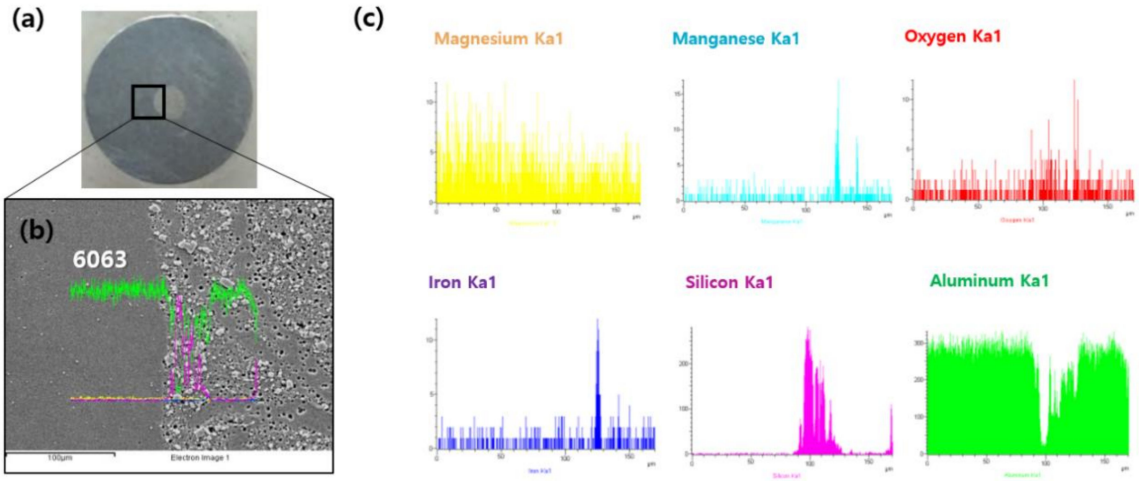

Figure 7. Elemental mapping of the area near the interface between Al6063 and Al3003. (**a**) Picture of a cross-section of the sample, (**b**) SEM image and mapping of all the elements, and (**c**) mapping of the major elements.

In general, while etching is conducted, the grain boundaries are oxidized more than the grain interior. Similarly, the interface is more corrosive due to the disordered arrangement of the atoms. To analyze the mechanical properties, Vickers hardness test and tensile test were conducted.

Figure 8 shows the Vickers hardness values measured on the cross section and longitudinal section of the FGM. The overall hardness in the transverse cross-section is observed to be in the range of 50–53 HV, which is almost 1.5 times greater than that generally observed for both Al3003-T0 and Al6063-T0, as shown in Table 2, and the hardness values are nearly constant. Al6063 has good corrosion resistance, and furthermore, it is fabricated in the bulk form; therefore, it is only slightly oxidized. The high hardness value of 53.03 HV observed at the interface confirms that the Al3003/Al6063 FGM has superior interface properties. Moreover, in the cross-section, although the hardness of the individual parts is slightly different, this difference is not large; therefore, the hardness is uniform.

However, the measured value of the hardness of the longitudinal section is relatively lower when compared to that of the transverse cross-section. This could be because the particle size is further reduced in the cross-section where the grains are subjected to a compressive pressure from all directions, which is less than that in the longitudinal cross-section. While joining two different materials, the properties of the joint play an important role—if the two materials are well bonded, the interfacial properties and the physical properties of the final product are improved.

In contrast, the longitudinal section is elongated in the direction of extrusion and the particles are compressed in a direction vertical to the direction of extrusion.

Table 2. General specifications of mechanical properties of Al6063 and Al3003 [16].

Sample	Density (g/cm^3)	Vickers Hardness (HV)	0.2% Offset Yield Strength (MPa)	Tensile Strength (MPa)	Elongation (%)
3003-T0	2.73	30	40	110	28
6063-T0	2.70	26	50	90	-
6063-T5		70	145	185	12

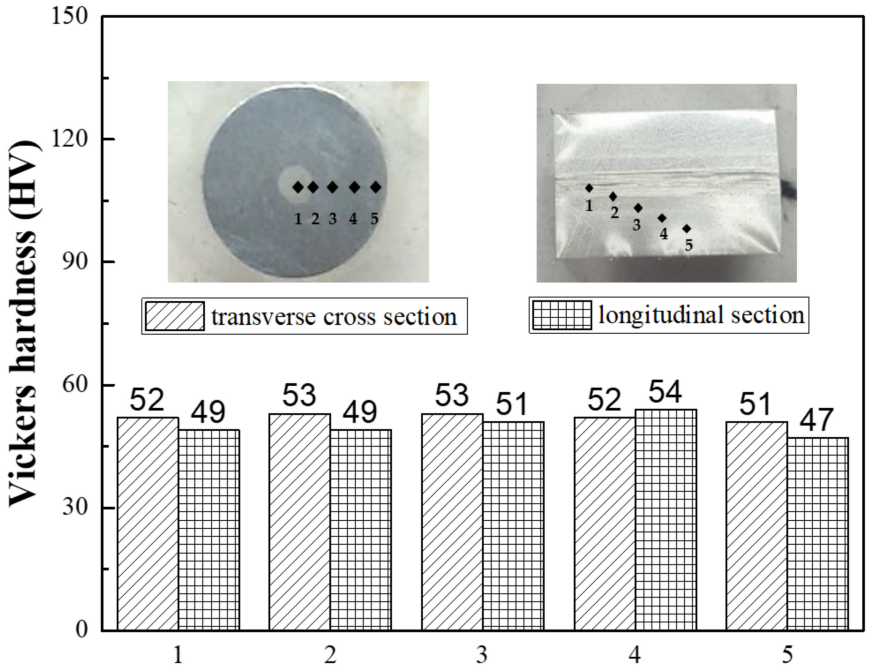

Figure 8. Vickers hardness graph measured on the transverse cross-section and longitudinal sections of the FGM at five regions from the center (Al3003) to Al6063, including the interface between Al3003 and Al6063.

Figure 9 shows the tensile stress–strain graph of the Al3003/Al6063 FGMs (T-0 and T-5). Al3003 and Al6063 have an area ratio of 18:82 at the neck of the tensile specimen. In the case of the T-0 Al3003/Al6063 FGM, the experimental tensile stress is improved to 152.19 MPa, as listed in Table 3, and in the case of the T-5 Al3003/Al6063 FGM, the general tensile stress is improved to 237.29 MPa, which is more than twice the generally observed average tensile stress values for Al3003 and Al6063, as shown in Table 2. The tensile stress of the material satisfies the T6 specification reported by Prillhofer et al. [17]. The elongation of the FGMs without heat treatment is more than 25%, which can solve the formability problem of the general aluminum 6000 series studied by Panigrahi et al. [18].

Furthermore, in the case of T-5 Al3003/Al6063 FGMs, the elongation, which is more than 10%, satisfies the abovementioned T6 specification. To analyze the strengthening mechanism, we considered two possible mechanisms: precipitation hardening and reduction of grain size. In the first mechanism, the precipitates present inside the matrix of the metal play a role in capturing dislocations, which increases the strength and hardness of the material.

Generally, Al alloys have precipitates and in the case of heat-treated alloys, the precipitates are formed and strengthened during the heat treatment. Pokov'a et al. showed that the α-$Al_{12\text{-}15}$ $(Fe, Mn)_3$ $Si_{1\text{-}2}$ phase and A_{l6} (Fe, Mn) phase are generally present in Al3003 [19], and Camero et al. reported that the precipitates in Al6063 such as Mg_2Si are generated mainly during heat treatment [20]. These precipitates serve to reinforce the material through a pinning effect. Furthermore, even if the amount and size of the precipitates are the same, the area of the FGMs is reduced by the extrusion process, which indicates that the proportion of the precipitate per unit area increases. Consequently, the movement of the dislocations is significantly inhibited; the strengthening of a material can occur through this mechanism. In the second mechanism, the materials are strengthened due to the reduction in grain size. As the crystal grain size of the material decreases, the grain boundary area increases in general, which disturbs the dislocation migration. Some researchers attempted to calculate the strength of the extruded materials using the Hall–Petch equation. For instance, Uematsu et al. showed that the grain size can be refined by controlling the extrusion conditions (extrusion ratio, working temperature), and showed that the Hall–Petch equation is valid for calculating the strength of the extruded alloys [21].

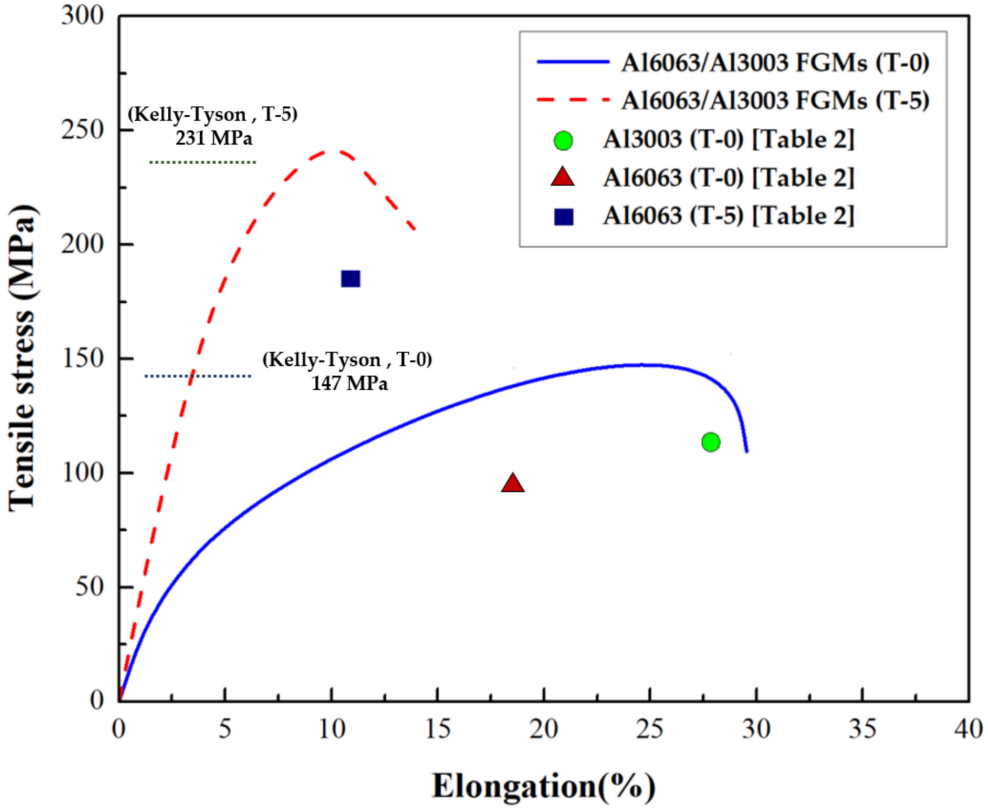

Figure 9. Stress and strain graph of Al3003/Al6063 FGMs (T-0 and T-5).

Furthermore, Kim et al. attempted to control the grain size using equal channel angular pressing, which is an extrusion method, and used the Hall–Petch equation to calculate the yield strength [22]. Thus, it can be concluded that the use of the Hall–Petch equation to calculate the extruded FGMs is valid, and hence, the equation was applied in this study.

To use the Hall–Petch equation, we first calculated the crystallite size by applying the Scherrer equation (Equation (1)). Some researchers applied the crystallite size to the grain size of the Hall-Petch equation, and proved that it is considerably valuable [23]. The Scherrer equation is expressed as follows [24]:

$$\tau = K\lambda/\beta\cos\theta \quad (1)$$

where τ is the mean size of the ordered (crystalline) domains, which may be smaller or equal to the grain size, and K is a dimensionless shape factor with a value close to unity. From the XRD data, the crystallite size of the Al3003 powder is determined to be 48.85 nm, while that of the Al3003/Al6063 FGM is determined to be 44.87 nm. It is thus confirmed that the grain size is decreased owing to the extrusion process and the result shows a possibility of strengthening due to the reduction in the grain size. The values of the crystallite sizes were substituted into the Hall–Petch equation to calculate the yield stress of Al3003 powder and Al3003/Al6063 FGM, as shown in Equation (2). The Hall–Petch equation is expressed as follows [21]:

$$\sigma = \sigma_0 + K_y d^{-1/2} \quad (2)$$

In this equation, σ_0 is the materials constant for the stress in the dislocation movement, K_y is the Hall–Petch slope, which is a strengthening coefficient, and d is the average grain size. It can be observed from this equation that the yield strength in the y-direction increases as the average particle size, d, decreases. In the case of the T-0 Al3003 sample, this effect caused by the reduction in particle size is expected to be observed through improving the material properties via solid-solution strengthening, dispersion strengthening, and work hardening. The value of σ_0 is approximately 58 MPa, while that of

s approximately K_y i96 MPa·μm$^{1/2}$, and the yield strength was calculated by substituting the crystallite size obtained from the Scherrer equation into the Hall–Petch equation.

The calculated value of the yield strength before extrusion is 491.92 MPa and that after extrusion is 511.12 MPa, showing an increase of approximately 20 MPa after the extrusion process. The strength of the final material is increased by ~50 MPa in the sample that was not subjected to the heat treatment. Additionally, precipitation hardening also plays a role in increasing the strength. Therefore, it is considered that a combined effect of these factors increases the final strength by 50 MPa.

Notably, the calculated value is much higher than the experimentally measured value. The considerable difference between the two values is possibly because of using the crystallite size instead of the actual grain size for the calculations. For instance, in the case of a polycrystalline material, the crystallite size is generally smaller than the grain size. If the strength were calculated using the actual grain size, which is expected to be larger than the crystallite size, in the Hall–Petch equation, the result is likely to be similar to the experimental value.

However, notably, the crystallite size was reduced after the extrusion process, and the difference between the strength of the raw materials and extruded materials is similar to the difference between the theoretical values calculated using the Hall–Petch equation. Therefore, the Hall–Petch equation is considered to be effective for explaining the tendency of the reduction in the grain size via the extrusion process and the relatively increased value of the strength. However, a more specific analysis is required to demonstrate the exact strengthening mechanisms, as there are possibly other strengthening factors besides the two factors mentioned in this paper.

To analyze the interactions between the increase in strength owing to the strengthening factors and the decrease in strength owing to the limitations (e.g., difficulty in atomic-level bonding of two other materials), further investigations in addition to quantitative and qualitative analytical data including simulations are required.

$$\sigma_y = \sigma_f V_f \left(1 - \frac{l_c}{2l}\right) + \sigma_m \left(1 - V_f\right) \quad (3)$$

Moreover, Kelly and Tyson established the equation for the yield strength of FGMs, in which the matrix and fiber are evenly mixed and aligned in a particular direction with perfect interfacial bonding [25].

Table 3. Experimental mechanical properties of Al6063/Al3003 FGM (T-0, T-5).

Sample		Bulk Density (g/cm3)	Relative Density (%)	Vickers Hardness (HV)	Diameter (mm)	0.2% Offset Yield Strength (MPa)	Tensile Strength (MPa)	Elongation (%)
Al6063/Al3003 functionally graded materials	T0	2.65 ± 0.00	98.26 ± 0.04	52.13 ± 1.03	8.0 ± 0.1	146.11 ± 0.01	152.19 ± 0.1	29.53 ± 1.99
	T5	2.65 ± 0.00	98.26 ± 0.04	75.00 ± 1.05	8.0 ± 0.1	236.79 ± 7.07	237.29 ± 6.57	13.87 ± 2.55

The Kelly–Tyson equation shows that the overall strength is improved by a load transfer to a fiber when a load is applied to a composite material produced by mixing a matrix and fiber, which indicates that the fiber serves as an enhancer. This equation is used for complex composites. When the material is produced through an extrusion process, the grains are elongated in a direction parallel to the extrusion direction, and the material is compressed in the vertical direction.

A previous study confirmed that this phenomenon actually occurs through the micrographs of the longitudinal cross-section of the Al-CNT composite produced via an extrusion process [26].

As shown in Figure 5a, when the pores distributed in Al3003 are examined, the particles are observed to be arranged in the direction of extrusion and the circular shape of the pores is elongated in the direction of the extrusion. Based on this observation, it was concluded that the Kelly–Tyson equation can be applied for the fabricated material used in this study.

Therefore, the Kelly–Tyson equation was employed, assuming that one material plays the role of the fiber and the other one plays the role of the matrix, although the two are not mixed in our case. Assuming that Al3003 is the matrix and Al6063 is the fiber, in the case of the T-0 FGM,

the calculated value of the strength is approximately 147 MPa, which is lower than the experimental value (152.19 MPa, as shown in Table 3). In the case of the heat-treated FGM T-5, the calculated value of the strength is expected to increase to approximately 231 MPa. This theoretical value is also lower than the experimental value for T-5 FGM (237.29 MPa, in Table 3). Thus, for both T-0 and T-5 FMGs, the experimental values are observed to be higher than the calculated values, although the difference is small (less than 5%). However, when the theoretical strength was calculated using the rule of mixtures equation, the values were 90.26 MPa (for T-0 FMG) and 183.32 MPa (for T-5 FMG). Thus, although the Al3003/Al6063 FGM fabricated in this study is not a perfectly mixed composite, it can be confirmed that the Kelly–Tyson equation can be applied to this system. Moreover, the higher experimental value indicates that there are additional factors, such as the reduction in particle size and precipitation hardening, which may play a significant role as described earlier.

The Kelly–Tyson equation considers strengthening effects only by fibers; therefore, this equation may not be the most appropriate equation in the present case. However, when considering all the different factors that affect the strengthening of the composites, this equation can be considered as most suitable.

4. Conclusions

The Al3003/Al6063 FGM was successfully fabricated via hot extrusion to realize multifunctionality including high strength and low weight.

The interface between the two materials is clear, with almost no cracks. It can be considered that the extruded FGM has excellent interface properties based on the high Vickers hardness of the interface. When the powder and bulk are in contact, the surface area of the contact could be larger than that between two bulks, so that the interface was improved.

The tensile strength of the final material subjected to T-5 heat treatment was observed to improve to twice that generally observed for Al3003 and Al6063, and the elongation was greater than 10%. From these results, it can be confirmed that the final product has a high strength and adequate elongation, which are the objectives of this study.

To analyze the strengthening mechanisms, i.e., precipitation hardening and grain refinement, strengthening via grain refinement was emphasized more in this study. Generally, the grain size of the powder is finer than the bulks and the presence of many grain boundaries hinders the grain growth. Therefore, the FGM fabricated using Al3003 powder could be strengthened by the fine grain size. Moreover, the grain size would be reduced by the extrusion process because the grains were subjected to mechanical stress. The Hall–Petch equation was used to explain the tendency for improved strength, which is appropriate for the explanation of the tendency of the increase in strength when the FGM was extruded; this was reported by earlier researchers, as well as observed in our study.

In addition, when the Kelly–Tyson equation was used assuming that Al6063 was a fiber, the theoretical results nearly corresponded to the experimental values. Therefore, the Kelly–Tyson equation could also be used to predict the strength of the extruded FGMs.

In summary, Al-alloy-based FGMs with lightweight and high strength properties were successfully fabricated via hot extrusion. Thus, it could be confirmed that hot extrusion is useful to fabricate FGMs with improved mechanical properties.

Author Contributions: D.K. and K.P. conducted the overall experiments; M.C., S.J., and S.H. fabricated materials via a hot extrusion process and conducted the heat treatment; the tensile test was conducted by S.C.; writing—original draft preparation, D.K.; writing—review and editing, H.K.; visualization, D.K.; supervision, H.K.; project administration, H.K.; and funding acquisition, H.K.

Funding: This research was funded by Ministry of SMEs and Startups (MSS).

Acknowledgments: This research was financially supported by the Ministry of SMEs and Startups (MSS), Korea, under the "Regional Specialized Industry Development Program" supervised by the Korea Institute for Advancement of Technology (KIAT), (2017_R0006154).

Conflicts of Interest: The authors declare no conflict of interest.

References

1. Kelkar, A.; Roth, R.; Clark, J. Automobile bodies: Can aluminum be an economical alternative to steel? *JOM* **2002**, *53*, 28–32. [CrossRef]
2. Park, K.; Park, J.; Kwon, H. Fabrication and characterization of Al-SUS316L composite materials manufactured by the spark plasma sintering process. *Mater. Sci. Eng. A* **2017**, *691*, 8–15. [CrossRef]
3. Morsi, K.; Esawi, A. Effect of mechanical alloying time and carbon nanotubes (CNT) content on the evolution of aluminum (Al)-CNT composite powders. *J. Mater. Sci.* **2007**, *13*, 4954–4959. [CrossRef]
4. Miyamoto, Y.; Kaysser, W.A.; Rabin, B.H.; Kawasaki, A.; Ford, R.G. *Functionally Graded Materials: Design, Processing and Applications, the Characterization of Properties*; Kluwer Academic Publishers: Boston, MA, USA; London, UK, 1999; pp. 89–160.
5. Watanabe, Y.; Inaguma, Y.; Sato, H.; Miura-Fujiwara, E. A novel fabrication method for functionally graded materials under centrifugal force: The centrifugal mixed-powder method. *Materials* **2009**, *2*, 2510–2525. [CrossRef]
6. Liu, T.; Wang, Q.; Gao, A.; Zhang, C.; Wang, C.; He, J. Fabrication of functionally graded materials by a semi-solid forming process under magnetic field gradients. *Scr. Mater.* **2007**, *57*, 992–995. [CrossRef]
7. Kwon, H.; Leparoux, M.; Kawasaki, A. Functionally graded dual-nanoparticulate-reinforced aluminum matrix bulk materials fabricated by spark plasma sintering. *J. Mater. Sci. Technol.* **2014**, *30*, 736–742. [CrossRef]
8. Vouler, T.J.; Clayton, J.D. Heterogeneous deformation and spall of an extruded tungsten alloy: Plate impact experiments and crystal plasticity modeling. *J. Mechanics and Physics of Solids* **2008**, *56*, 297–335. [CrossRef]
9. Cocen, U.; Onel, K. Ductility and strength of extruded SiCp/aluminum-alloy composites. *Comp. Sci. and Technol.* **2002**, *62*, 275–282. [CrossRef]
10. Fan, X.; Chen, L.; Chen, G.; Zhao, G.; Zhang, C. Joining of 1060/6063 aluminum alloys based on porthole die extrusion process. *J. Mater. Process. Technol.* **2017**, *250*, 65–72. [CrossRef]
11. Kwon, H.; Leparoux, M. Hot extruded carbon nanotube reinforced aluminum matrix composite materials. *Nanotechnology* **2012**, *23*, 415701. [CrossRef]
12. Uehara, K.; Sakurai, M. Bonding strength of adhesives and surface roughness of joined parts. *J. Mater. Process. Technol.* **2002**, *127*, 178–181. [CrossRef]
13. William, H.C. *Metals Handbook Vol. 4: Heat Treating*, 9th ed.; American Society for Metals: Metals Park, OH, USA, 1981; p. 216.
14. 3003 (AlMn1Cu, 3.0517, A93003) Aluminum. Available online: https://www.makeitfrom.com/material-properties/3003-AlMn1Cu-3.0517-A93003-Aluminum (accessed on 13 August 2018).
15. Alcoa. Alloy 6063 Datasheet. Available online: https://web.archive.org/web/20031006212043/http://www.alcoa.com/adip/catalog/pdf/Extruded_Alloy_6063.pdf (accessed on 1 November 2006).
16. Kaufman, J.G. Properties of Aluminum Alloys: Fatigue Data and the Effects of Temperature, Product Form, and Processing. ASM International: Metal Park, OH, USA, 2008; pp. 9–17.
17. Prillhofer, R.; Rank, G.; Berneder, J.; Antrekowitsch, H.; Uggowitzer, P.J.; Pogatscher, S. Property criteria for automotive Al-Mg-Si sheet alloys. *Materials* **2014**, *7*, 5047–5068. [CrossRef] [PubMed]
18. Panigrahi, S.K.; Jayaganthan, R.; Pancholi, V. Effect of plastic deformation conditions on microstructural characteristics and mechanical properties of Al 6063 alloy. *Mater. Des.* **2009**, *30*, 1894–1901. [CrossRef]
19. Pokov´a, M.; Cieslar, M.; Lacaze, J. Enhanced AW3003 aluminum alloys for heat exchangers. *WDS* **2011**, *11*, 141–146.
20. Camero, S.; Puchi, E.S.; Gonzalez, G. Effect of 0.1% vanadium addition on precipitation behavior and mechanical properties of Al-6063 commercial alloy. *J. Mater. Sci.* **2006**, *41*, 7361–7373. [CrossRef]
21. Uematsu, Y.; Tokaji, K.; Kamakura, M.; Uchida, K.; Shibata, H.; Bekku, N. Effect of extrusion conditions on grain refinement and fatigue behaviour in magnesium alloys. *Mater. Sci. Eng. A* **2006**, *434*, 131–140. [CrossRef]
22. Kim, W.J.; An, C.W.; Kim, Y.S.; Hong, S.I. Mechanical properties and microstructures of an AZ61Mg Alloy produced by equal channel angular pressing. *Scr. Mater.* **2002**, *47*, 39–44. [CrossRef]
23. Ong, C.Y.A.; Blackwood, D.J.; Li, Y. The effects of W content on solid-solution strengthening and the critical hall-petch grain size in Ni-W alloy. *Surf. Coat. Technol.* **2019**, *357*, 23–27. [CrossRef]

24. Monshi, A.; Foroughi, M.R.; Monshi, M.R. Modified scherrer equation to estimate more accurately nano-crystallite size using XRD. *World J. Nano. Sci. Eng.* **2012**, *2*, 154–160. [CrossRef]
25. Kelly, A.; Tyson, W.R. Tensile properties of fibre-reinforced metals: Copper/tungsten and copper/molybdenum. *J. Mech. Phys. Solids* **1965**, *13*, 329–350. [CrossRef]
26. Kwon, H.; Estili, M.; Takagi, K.; Miyazaki, T.; Kawasaki, A. Combination of hot extrusion and spark plasma sintering for producing carbon nanotube reinforced aluminum matrix composites. *Carbon* **2009**, *47*, 570–577. [CrossRef]